# EXPERIMENTAL CHARACTERIZATION AND MODELING FOR EQUIVALENCE RATIO SENSING IN NON-PREMIXED FLAMES USING CHEMILUMINESCENCE AND LIBS TECHNIQUES

*Laura Merotto[a*], Mariano Sirignano[b], Mario Commodo[c], Andrea D'Anna[b], Roberto Dondè[a], and Silvana De Iuliis[a]*

[a] Istituto di Chimica della Materia Condensata e di Tecnologie per l'Energia CNR-ICMATE, Milano, Italy

[b] Dipartimento di Ingegneria Chimica, dei Materiali e della Produzione Industriale, Università degli Studi di Napoli Federico II, Napoli, Italy

[c] Istituto di Ricerche sulla Combustione, CNR-IRC, Napoli, Italy

*Corresponding Author: Laura Merotto (merotto@icmate.cnr.it)

**Keywords**

LIBS, chemiluminescence, diffusion flames, experimental and modeling

**Abstract**

Real-time monitoring of local equivalence ratio is of primary importance for combustion efficiency improvement. Chemiluminescence and laser induced breakdown spectroscopy (LIBS) measurements can be powerful tools for sensing equivalence ratio. Radicals such as OH*, CH*, and $C_2$* are formed within the flame front and consequently the related chemiluminescence emission can be considered as a marker to follow the evolution of combustion processes. From LIBS measurements, the ratio of two characteristic spectral lines of fuel (H) and oxidizer (O) is related to the equivalence ratio. In this work, LIBS measurements have been carried out in premixed flames of known equivalence ratio for calibration purposes. Then, the application to non-premixed flames has been performed to evaluate the local equivalence ratio. Chemiluminescence emission spectra have been also collected and the values of the OH*, CH* and $C_2$* have been properly evaluated taking into account the contribution of $CO_2$* broad band emission. A methane co-flow diffusion flame has been investigated along the centerline as well as at three cross sections and the local equivalence ratio profiles obtained by LIBS have been compared with CH* chemiluminescence profiles. Finally, the experimental data obtained were compared to the results of a detailed chemical kinetic model.

## 1. Introduction

Energy efficiency monitoring and environmental impact are of major importance in conventional as well as in innovative combustion systems. The local equivalence ratio, $\phi$, is a

significant parameter able to give information on local mixing between fuel and oxidizer and consequently on energy conversion efficiency both in steady state and transient regime combustion systems. Local ϕ evaluation is mandatory to identify reactor configurations promoting the optimal fuel/oxidizer mixing and thus the complete energy conversion [1].

Flame chemiluminescence spectroscopy is a promising tool for equivalence ratio monitoring, due to its simplicity when compared to laser based diagnostics [2-7]. The chemiluminescence emission of radical species occurs when such radicals return from an excited to a lower energy state, thus emitting light at characteristic wavelengths. Radicals such as OH*, CH* and $C_2$* are chemically formed within the flame and generally used to evaluate the evolution of the combustion process. Chemiluminescence of these species can be indicative of the reacting conditions in the flame: in particular from chemiluminescence intensity it is possible to track the heat release [4,9] in the flame and from the ratio of emission from excited species, such as CH*/OH* or $C_2$*/CH*, it is possible to evaluate the evolution of the equivalence ratio at the investigated conditions [2, 10, 11].

In addition to chemiluminescence measurements an interesting approach to evaluate the local equivalence ratio is the laser-induced breakdown spectroscopy (LIBS) [12-14]. This technique is based on focusing a pulsed laser beam into a spot and producing a plasma; the local electric field intensity is high enough to atomize and ionize molecules and atoms in the probe volume, which recombine and then relax, emitting a characteristic emission intensity at given wavelengths. From the emission spectral analysis, information about the elemental composition of the sample can be derived. Considering the application in a hydrocarbon combustion system, typical H, O, C spectral lines can be easily detected [15]. As reported in literature, the ratio of two characteristic spectral lines of fuel and oxidizer (H/O and C/O) is related to the equivalence ratio [13-18].

Although LIBS and chemiluminescence have been already adopted to investigate combustion systems, few works are reported in literature on the comparison and/or coupling of the two techniques with the aim to investigate the applicability for a reliable equivalence ratio evaluation [19-22]. In Tripathy et al. [19] a multivariate approach has been proposed for LIBS and chemiluminescence measurements performed in a methane/air premixed flame. LIBS-based calibration was proved to provide better predictions of equivalence ratios compared to the chemiluminescence-based calibration. Furthermore, although these techniques have been widely applied in premixed flames, the vast majority of flames used in industrial and practical applications are non-premixed, thus local equivalence ratio measurements in diffusion flames are of major interest. To our knowledge, few works concerning the application of LIBS technique in diffusion flames for local equivalence ratio evaluation are reported in the literature [17, 18, 20-22]. In these works this evaluation has been derived by using the equivalence ratio calibration obtained in the premixed flame or as in Ref. [21] by assuming a relationship between the fuel mass fraction and the equivalence ratio.

In the present work the assessment of the applicability of LIBS and chemiluminescence measurements for local equivalence ratio sensing in a diffusion flame has been taken into account. In particular, calibration measurements have been carried out in methane/air premixed flames to obtain calibration curves of the LIBS signal ratio as a function of the equivalence ratio. This calibration has been applied to LIBS measured performed in a methane diffusion flame and the local equivalence ratio values obtained compared with chemiluminescence results. These experimental results are also compared to numerical data derived from a detailed kinetic model of the flame.

## 2. Materials and Methods

### *2.1 Experimental set up*

The experimental apparatus for chemiluminescence and LIBS measurements is shown in Figure 1. In order to perform chemiluminescence measurements, a section of the flame was imaged with a magnification of 3 on a 1 mm pinhole by using an achromatic lens (f = 100 mm), to increase chemiluminescence emission detection against the background flame luminosity. The radiation emitted from the flame was then imaged onto an optical fibre by using an achromatic lens (f = 100 mm) with 1:1 magnification. The fibre was connected to the entrance slit of a spectrograph (ANDOR Technology Shamrock 303i) coupled with an ICCD camera (iStar 334T). The spectra were collected by using a 150 grooves/mm grating (0.28 nm resolution) in the spectral range of 200 nm – 600 nm.

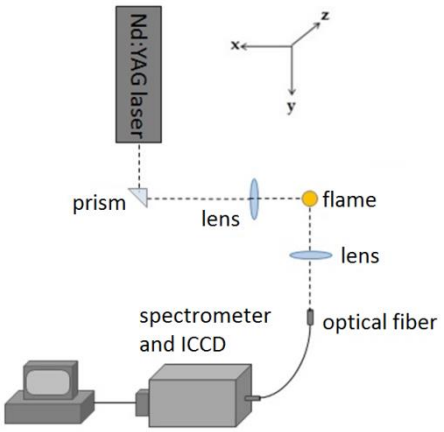


**Figure 1.** Chemiluminescence and LIBS measurements setup.

A typical chemiluminescence spectrum is reported in Fig. 2. In the same figure, the peaks of OH* (λ=310 nm), CH* (λ =430 nm) and $C_2$* (λ =516 nm) radical chemiluminescence emission can be easily identified, overlapped on a continuum band due to $CO_2$* chemiluminescence

emission [2]. As already observed, thanks to the particular experimental configuration used, the contribution of radicals emission is significant compared to the continuum $CO_2$* intensity.

The measurement of the chemiluminescence signal has been performed taking the integral of the whole emission band with the subtraction of the underlying background. Chemiluminescence spectra resulted from the average over 100 acquisitions.

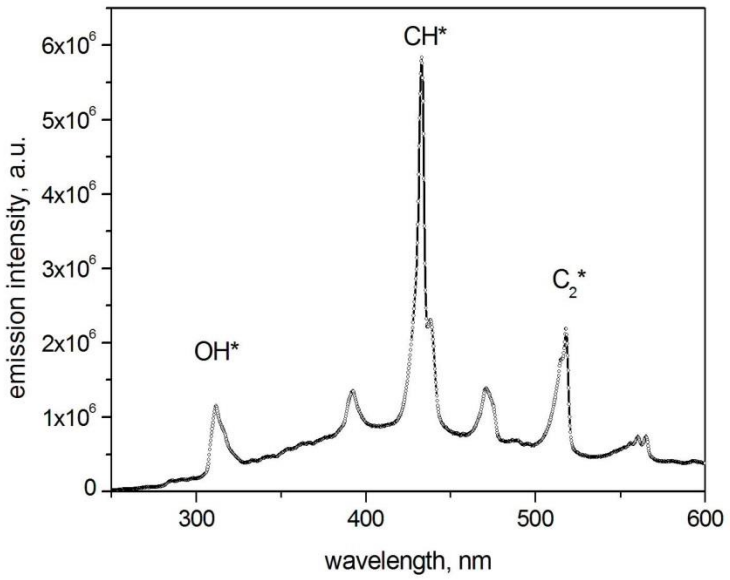


**Figure 2**. Typical spectrum of chemiluminescence. Emissions peaks of OH*, CH* and $C_2$* radicals are indicated.

For LIBS measurements, a pulsed Nd:YAG laser (Quanta System, 7 ns FWHM) at the fundamental wavelength (1064 nm), with 1 Hz repetition rate and 220 mJ pulse energy was used to produce the plasma by focusing the beam with a 80 mm focal length lens. The detection system was the same implemented for chemiluminescence measurements. Each LIBS spectrum resulted

from the average over 100 acquisitions in order to increase the signal to noise ratio and were collected with a 1 μs delay time with respect to the laser pulse and a 1 μs detection gate width.

In the presence of hydrocarbon fuels and air, C, H, O and N are the only atomic species in the probe volume. A typical LIBS spectrum is shown in Fig. 3. In this work H (656 nm) and O (777 nm) are taken into account as representative of fuel and oxidizer, respectively. The ratio of these two elements, in fact, has been proven to be more sensitive to equivalence ratio [17] when compared to the ratio of other radical emissions. The adopted experimental conditions allow increasing LIBS signal detection again the continuum plasma emission, which becomes lower and lower with the delay time. The LIBS signal has been evaluated by measuring the integral of the peak (both H and O lines) and subtracting the related background. Considering an average over 100 spectra, the uncertainty of the LIBS signal is about 3% resulting in an uncertainty in the H/O ratio of about 3%.

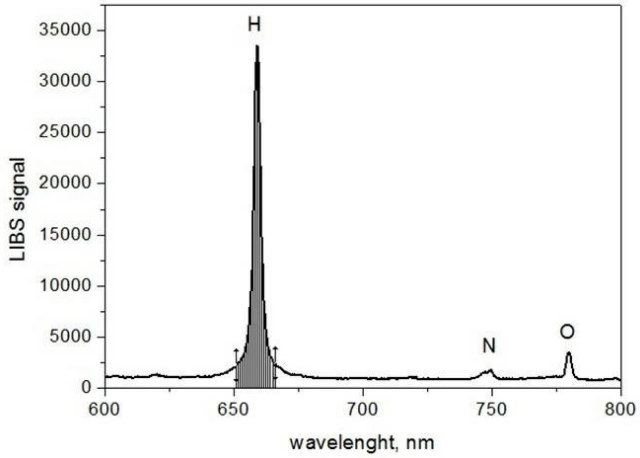


**Figure 3**. Typical LIBS emission intensity vs. wavelength.

For calibration purposes, a series of methane/air premixed flames were analysed. The flames were stabilized on a burner, consisting of two concentric brass tubes (10 mm I.D., 100 mm O.D.)

by keeping constant the total mass flow rate ($5.3x10^{-5}$ kg/s) and varying the equivalence ratio from 0.9 to 1.5. The same burner was used for both premixed and non-premixed flames investigation [23-26].

In Figure 4 H/O intensity ratios of LIBS signal measured in premixed methane/air flame are reported as a function of equivalence ratio. As a result, a power trend $H/O = 9.81 \cdot \phi^{0.89}$, was obtained with a determination coefficient of $R^2$=0.9995.

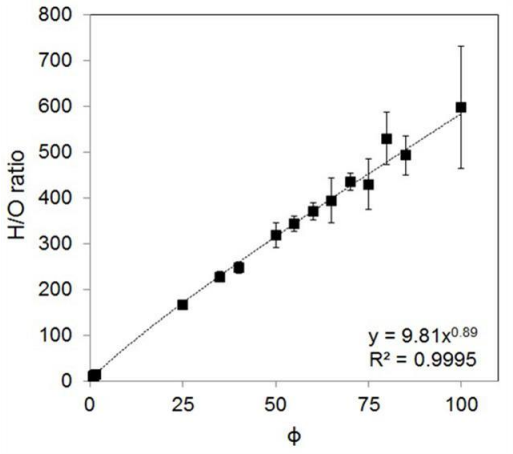


**Figure 4**. H/O LIBS intensities ratio vs. equivalence ratio.

Once the calibration curve was acquired, systematic measurements were carried out on a methane diffusion flame stabilized on the same burner. The methane mass flow rate sent in the inner tube was fixed at $5.9x10^{-6}$ kg/s, resulting in a gas velocity of 11.46 cm/s at standard temperature and pressure and producing a 28 mm total height flame. Stabilization of the diffusion flame was achieved by flowing $1.4x10^{-3}$ kg/s air in the external tube of the co-flow burner. Methane and air flow rates are controlled with regulated mass flow meters (Bronkhorst, AK Ruurlo, The Netherlands).

Temperature measurements were performed in the investigated co-flow diffusion flame using a 127 μm Pt/Pt-Rh(10%) thermocouple. In flame regions where soot particles are present, to account for the soot deposition on the thermocouple bead, resulting in significant radiant losses and flame temperature underestimation, a rapid insertion procedure is performed as reported in [27]. The temperature at a certain height above the burner is measured by a rapid transversal insertion of the thermocouple in the flame and the maximum value is taken before the radiative losses become significant. Temperature values are corrected for radiation losses following the literature procedures [28].

### *2.2 Chemical kinetic modeling*

Hydrocarbon oxidation and pyrolysis are described by a detailed kinetic mechanism able to model several premixed and diffusion flames at atmospheric pressure. The detailed gas-phase kinetic mechanism is built onto the GRI-Mech 3.0 for C1 and C2 species [29] and the Miller and Melius mechanism for C3 and C4 species [30]. It considers the sequential addition of acetylene molecules and the self-combination of resonantly stabilized radicals to account for the molecular growth of aromatic cycles up to pyrene [31-33]. The model is also able to follow the molecular growth and the formation of aromatic compounds towards soot. In the present work soot was not modeled, and pyrene is the largest compound considered. The influence of soot on the local equivalence ratio in this flame was evaluated as of a minor importance. The gas-phase kinetic mechanism consists of 460 reactions involving 120 species and has been used for the gas phase was the same used in previous works [34-37].

Gas-phase transport equations (continuity, axial momentum, radial momentum, species' mass fractions and enthalpy) are solved for steady-state axisymmetric conditions. Radiation is modeled

as broadband without scattering and the absorption coefficient was set by matching the predicted with the experimental peak temperature. Diffusivities are taken from Chemkin [38]; they are binary coefficients in nitrogen; the viscosity and thermal conductivity of the mixture are likewise those for nitrogen.

The transport equations are solved by a finite volume numerical method using a first order advective scheme [34]. The computational domain was 10 cm axial by 10-cm diameter, which is sufficiently large for the downstream exit and the radial outer boundary not to influence the flame field. An embedded grid is used in the base grid to obtain cell sizes of 0.2-mm axial and 0.1-mm radial in regions of high gradients, typically near the burner. The base grid cells are of variable size, typically 0.5-mm axial and 0.3-mm radial near the burner. The effect of grid fineness is tested by halving the cell size in the axial and radial directions. The computations performed with different grids show no significant difference for the centerline temperature profile.

## 3. Results Discussion

The equivalence ratio $\phi$ is defined for premixed flames as the actual weight ratio between fuel and oxidizer divided by the weight stoichiometric ratio. This definition is valid until the reaction does not occur. In general, when a reaction is involved, the concept of mixture fraction is introduced. However, it is common in literature to maintain $\phi$ as parameter, by defining it as local equivalence ratio. Nevertheless, some distinctions have to be made. When, as in this case, pure diffusion flames are considered, fuel and oxidizer are not mixed being the combustion processes due to the inter-diffusion of the two species. Consequently, the presence of oxygen in the fuel region is due to the diffusion of combustion products. The same origin has the presence of fuel atomic species in the oxidizer region. Therefore, in this case the measured local $\phi$ given by LIBS

actually describes the dilution of either fuel or oxidizer by the combustion products originating in the reaction zone. When the mixing mechanism is not limited to pure diffusion and turbulence plays an important role in creating local pockets of unburned fuel/oxidizer mixture, care has to be taken in the local ϕ meaning. In fact, the local ϕ has again the same meaning as the premixed case definition only until reaction does not occur and until combustion products recirculation is not present.

Local ϕ can be defined using, instead of the fuel and oxidizer mass ratio, the mass ratio of the atomic species derived from fuel and those derived from the oxidizer [39], and can therefore be evaluated from measured species concentration. In the present work, H and O atoms are measured using LIBS. As LIBS does not distinguish the molecule these atoms belong to, the H/O ratio measured is likely to include H and O from products as well as from reactants. Thus, the ϕ definition coincides with the above mentioned one [39].

In Fig. 5 the measured temperature profile along the centerline in the 28 mm diffusion methane flame is reported. Modeled results are also reported for comparison. A maximum temperature of about 1900 K is obtained at approximately 25 mm from the nozzle exit. The comparison between experimental results and those modeled is shown in good agreement.

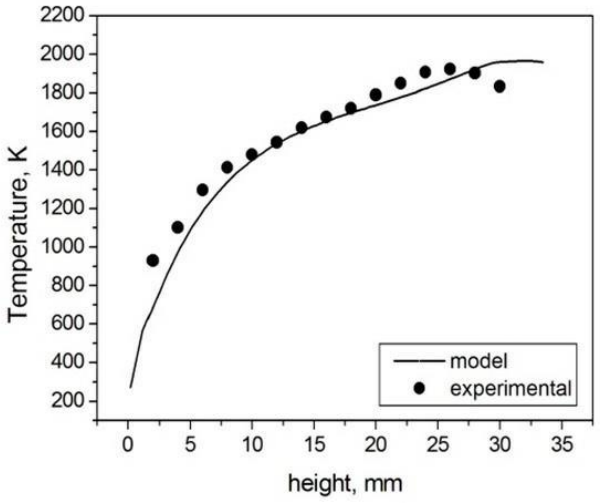


**Figure 5**. Measured and modeled centerline flame temperature.

The local equivalence ratio ϕ, evaluated from H/O LIBS measurements with the calibration curve, along the centerline of the methane diffusion flame is reported in Fig. 6, together with modeled results. The local fuel/air ratio significantly decreases with the height above the burner, reaching the stoichiometric value close to the flame tip. Experimental and numerical results are in good agreement, showing the potential of the LIBS technique in following the evolution of the combustion process from the early stage to the end of the flame.

In addition to LIBS measurements, the local equivalence ratio evaluation in the laminar diffusion flame has been investigated by using chemiluminescence emission spectroscopy. Chemiluminescence measurements in the coflow diffusion flame have to be considered integrated along the line of sight. In order to obtain local values, a mathematical inversion procedure (Abel transform) has been applied [40]. Radial profiles of chemiluminescence signals were obtained with a spatial resolution of 500 μm in the methane diffusion flame at 2.5, 5 and 10 mm height above the burner (HAB).

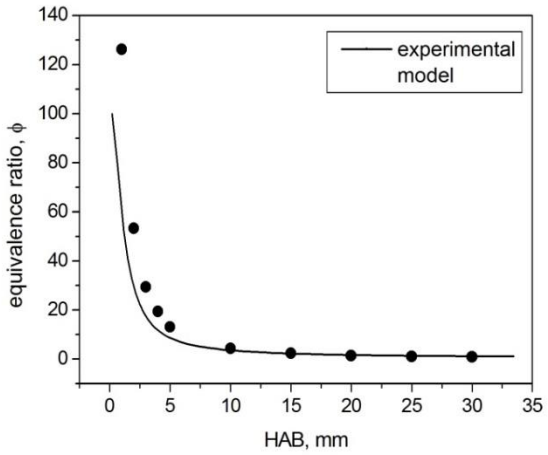


**Figure 6**. Axial profile of the equivalence ratio from LIBS.

Local CH*, OH* and $C_2$* chemiluminescence signals are plotted versus the distance from the flame axis in Figures 7a, 7b and 7c, respectively.

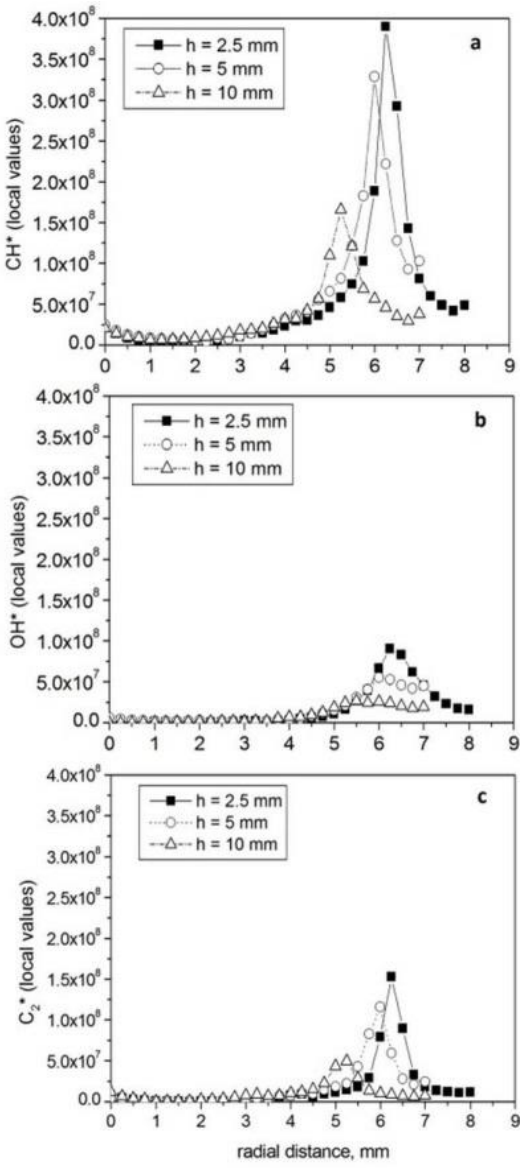


**Figure 7.** CH* (a), OH* (b) and $C_2$* (c) intensities (local values) at different heights in flame.

As it can be seen in the figure, chemiluminescence signal is close to zero in the inner part of the flame and exhibits a peak in the external annular region. Moving upward in the flame, the peak becomes lower and shifted towards the flame axis, following the closure of the flame. Comparing the three radical emissions, the maximum chemiluminescence value occurs approximately at the

same radial location in the flame. The small fluctuations detected on the flame axis have to be attributed to the mathematical error induced by the Abel inversion procedure applied.

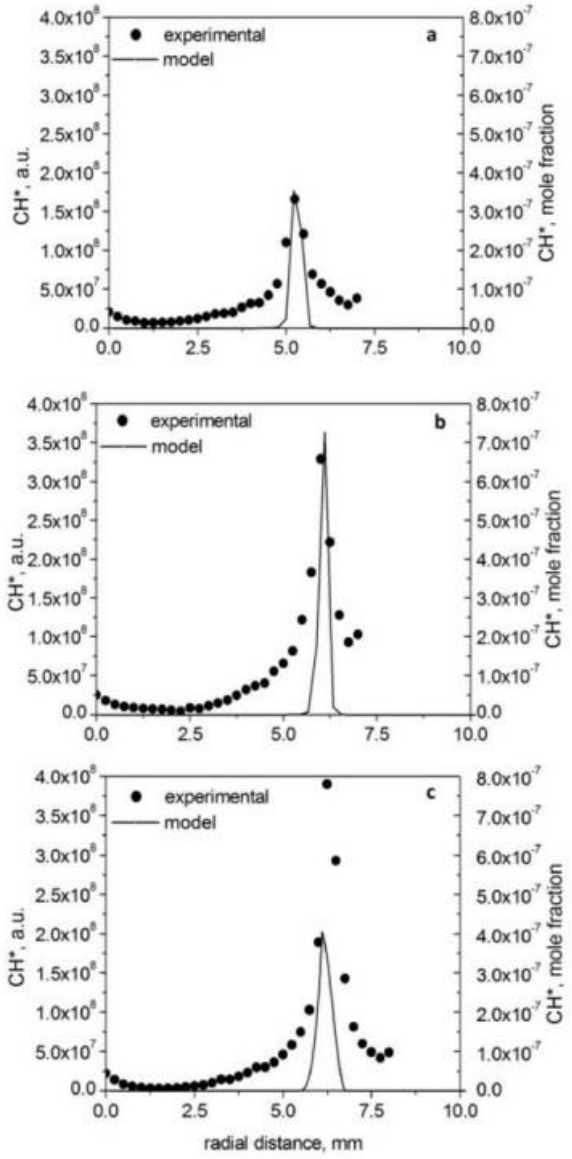


**Figure 8.** Experimental and modeled CH* values at heights = 10 mm (a), 5 mm (b) and 2.5 mm (c).

The measured CH* intensities were compared to the modeled CH* mole fractions, for the three heights investigated, and results are reported in Fig. 8. A good agreement between experimental and numerical results is obtained in all cases. In particular the model well predicts the position of the peak for the CH* radical and slightly over predicts the relative intensity at 10 mm above the burner.

LIBS measurements have been performed radially across the flame with a 0.5 mm step at the same heights above the burner as the chemiluminescence measurements, 2.5, 5 and 10 mm. The resulting H/O LIBS intensity ratio profiles along the radius of the flame are reported in Figure 9. It can be seen that at each height, H/O ratio increases moving from the external to the inner part of the flame. By using the calibration curve obtained from the premixed flame, shown in Figure 4, the local equivalence ratio ($\phi$) in the three different sections in the diffusion flame can be evaluated.

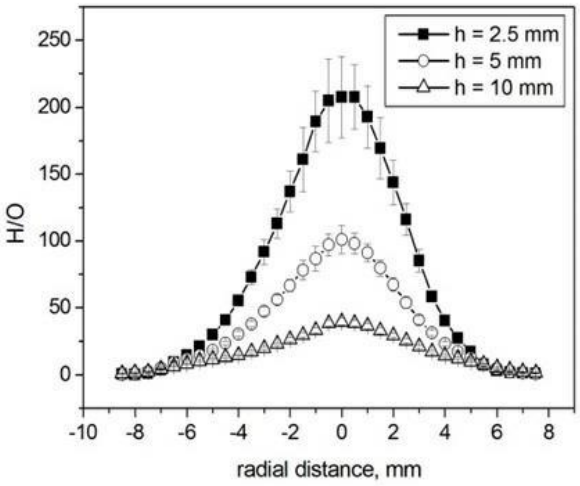


**Figure 9**. H/O ratio vs. distance from burner center, for the three heights investigated.

In order to compare LIBS and chemiluminescence measurements, the equivalence ratio obtained from LIBS measurements are reported in Figure 10 together with the CH* chemiluminescence signal across the three heights investigated.

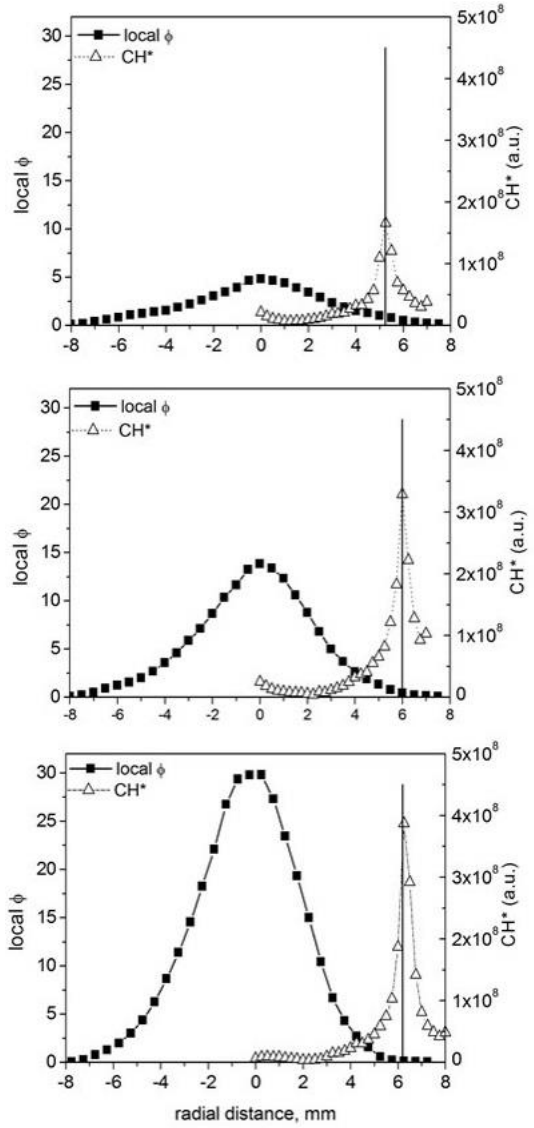


**Figure 10**. Local Φ calculated for diffusion flame and CH* signal vs. distance from the burner center. Heights = 10 mm (a), 5 mm (b) and 2.5 mm (c).

For each radial profile, the maximum CH* chemiluminescence signal, highlighted with a vertical bar in the figures, occurs in the flame position in which the local ϕ is close to 1. Chemiluminescence and LIBS values are discrete, therefore the flame front position can be evaluated with a resolution of 0.25 mm.

In particular, at HAB = 10 mm (Fig. 10a), LIBS measurements show that the local ϕ is 1.08 at 5 mm from the centerline, and 0.82 at 5.5 mm. By linearly interpolating the data, it is found that ϕ equals 1 at 5.16 mm. Chemiluminescence results (having a resolution of 0.25 mm) show a CH* maximum located at 5 mm from the centerline, and the modeled result is 5.22. For HAB = 5 mm (Fig. 10b), CH* has a maximum at 6 mm from the centerline. The corresponding modeled value is 6.11 mm. LIBS data interpolation gives ϕ =1 at 6.35 mm. For HAB = 2.5 mm (Fig. 10c) the maximum CH* obtained with chemiluminescence measurements falls at 6.25 mm from the centerline, while the modeled result is 6.11 mm. LIBS data interpolation gives 6.44 mm.

These results allow to infer that the LIBS signal ratio properly calibrated can be used as a powerful tool to obtain local equivalence ratio in a diffusion flame.

As already observed in the introduction, chemiluminescence emission ratios (OH*/CH* and $C_2$*/CH*) have been proved to be used for sensing equivalence ratio in the premixed flames. Results in premixed flames (not reported here) show the linear trend of the chemiluminescence signals ratio versus the equivalence ratio are in good agreement with literature data [41]. An interesting topic is to assess the applicability of this kind of analysis to a diffusion flame, that is the investigation of the applicability of the chemiluminescence signals ratio for sensing local equivalence ratio in a diffusion flame by using the calibration obtained from premixed flames. Unfortunately, this approach seems not to be suitable. In fact, at a given height above the burner

by taking the ratio of the CH* and OH* emission intensities in the diffusion flame and the derived equivalence ratio, these results do not match with the values obtained from LIBS measurements. Furthermore, the stoichiometric value obtained with chemiluminescence does not occur at the maximum of CH* position. Such a result can be attributed to different combustion pathways and temperature gradient obtained in diffusion and premixed flame. Therefore, while the chemiluminescence signal can be used for localize the region where the combustion processes occur even in the diffusion flame, the evaluation of the local equivalence ratio can not be obtained with chemiluminescence signals ratio. In non-premixed configuration, however, local equivalence value can be suitably obtained by using LIBS measurements.

Finally, as a further observation, LIBS measurements allow obtaining the local equivalence ratio even in the zones where no reaction occurs, e.g., in pyrolytic conditions and/or close to the fuel nozzle.

## 4. Conclusions

Chemiluminescence and LIBS measurements have been carried out in methane/air premixed and diffusion flames in order to evaluate the possibility to use these techniques to give information on the local equivalence ratio. Detailed flame modeling was also performed and compared with experimental data. In the diffusion flame, the local equivalence ratio was obtained from LIBS measurements using the calibration performed in the premixed flame. The evolution of the local equivalence ratio evaluated with LIBS along the centerline was in good agreement with the indication about the length of the flame derived from temperature measurements and with modelling results.

The location of the stoichiometric conditions along the radius measured with LIBS were in agreement with the position of the OH*, CH* peaks measured by chemiluminescence spectroscopy.

Due to the strong sensitivity to the temperature and $CO_2$ concentration, chemiluminescence measurements cannot be performed in every location of the flame. In contrast LIBS measurements can be performed regardless of the local temperature or mixing and thus are very promising for the local equivalence ratio evaluation and generally for the investigation of the mixing processes.

**Acknowledgements**

This work was financially supported by Accordo MSE-CNR - Ricerca di sistema elettrico nazionale - Project "Miglioramento dell'efficienza energetica dei sistemi di conversione locale di energia" PAR 2013-2014.

**References**

[1] J. Ballester, T. Garcia-Armingol, Diagnostic techniques for the monitoring and control of practical flames Progress in Energy and Combustion Science 36.4: 375-411 (2010).

[2] J. Kojima, Y. Ikeda, T. Nakajima, Spatially resolved measurements of OH*, CH*, and $C_2$* chemiluminescence in the reaction zone of laminar methane/air premixed flames, Proc. Combust. Inst. 28: 1757-1764 (2000).

[3] F. Migliorini, S. Maffi, S. De Iuliis, G. Zizak, Analysis of chemiluminescence measurements

by grey-scale ICCD and Colour digital cameras, Meas. Sci. Technol. 25: 55202-55209 (2014).

[4] Y. Hardalupas, M. Orain, Local measurements of the time-dependent heat release rate and equivalence ratio using chemiluminescence emission from a flame, Combust. Flame 139.3: 188-207 (2004).

[5] Y. Ikeda, J. Kojima, H. Hashimoto, Local chemiluminescence spectra measurements in a high-pressure laminar methane/air premixed flame, Proc. Combust.Inst. 29(2): 1495-1501 (2002).

[6] R. J. Roby, J. E. Reaney, E. L. Johnsson, Detection of temperature and equivalence ratio in turbulent premixed flames using chemiluminescence. Virginia Polytechnic Inst. and State Univ., Blacksburg (US) (1998).

[7] C. S. Panoutsos, Y. Hardalupas, A.M.K.P. Taylor, Numerical evaluation of equivalence ratio measurement using OH* and CH* chemiluminescence in premixed and non-premixed methane–air flames, Combust. Flame 156(2): 273-291 (2009).

[8] F.V. Tinaut, M. Reyes, B. Giménez, and J.V. Pastor (2010), Measurements of OH* and CH* chemiluminescence in premixed flames in a constant volume combustion bomb under autoignition conditions. Energy & Fuels, 25(1), 119-129.

[9] M. Lauer, and T. Sattelmayer, Heat release calculation in a turbulent swirl flame from laser and chemiluminescence measurements. 14th International Symposium on Applications of Laser Techniques to Fluid Mechanics, Lisbon, Portugal, July. (2008).

[10] V. Nori, and J. Seitzman, Chemiluminescence measurements and modeling in syngas, methane and jet-A fueled combustors. 45th AIAA Aerospace Sciences Meeting and Exhibit, Reno, NV, January 2007.

[11] V. Nori, and J. Seitzman, Evaluation of chemiluminescence as a combustion diagnostic under varying operating conditions. AIAA paper 953 (2008).

[12] P. Stavropoulos, A. Michalakou, G. Skevis, S. Couris, Global and Local Equivalence Ratio Measurements in Laminar Premixed Hydrocarbon-Air Flames using Laser Induced Breakdown Spectroscopy (LIBS), Proceedings of the European Combustion Meeting, 2005.

[13] P. Stavropoulos, A. Michalakou, G. Skevis, S. Couris, Quantitative local equivalence ratio determination in laminar premixed methane-air flames by laser induced breakdown spectroscopy (LIBS), Chemical Physics Letters 404, 4-6: 309-314 (2005).

[14] P. Stavropoulos, A. Michalakou, G. Skevis, S. Couris, Laser-induced breakdown spectroscopy as an analytical tool for equivalence ratio measurement in methane–air premixed flames, Spectrochim. Acta B:, 60(7): 1092-1097 (2005).

[15] S. Zhengjie, Y. Hardalupas, and A. M. K. P. Taylor, Local Equivalence Ratio Measurement in Opposed Jet Flames of Premixed and Non-Premixed Methane-Air Using Laser-Induced Breakdown Spectroscopy, 18th Int. Symposium on the Application of Laser and Imaging Techniques to Fluid Mechanics, Lisbon Portugal, July 4 – 7, 2016.

[16] J. Kiefer, W.T. Johannes, L. Zhongshan, T. Seeger, M. Alden, A. Leipertz, Laser-induced breakdown flame thermometry, Combust. Flame 159.12: 3576-3582 (2012).

[17] J. Kiefer, J. W. Troger, Z.S. Li, M. Alden, Laser-Induced plasma in methane and dimethyl ether for flame ignition and combustion diagnostics, Appl. Phys. B 103: 229-236 (2011).

[18] M. Kotzagianni, R. Yuan, E. Mastorakos, and S. Couris, (2016). Laser-induced breakdown spectroscopy measurements of mean mixture fraction in turbulent methane flames with a novel calibration scheme. *Combustion and Flame*, *167*, 72-85.

[19] M.M. Tripathi, KK. Srinivasan, S.R. Krishnan, F.Y. Yueh, J.P. Singh, A comparison of multivariate LIBS and chemiluminescence-based local equivalence ratio measurements in premixed atmospheric methane–air flames, Fuel, 106: 318-326 (2013).

[20] T.X. Phuoc, F.P. White, Laser-induced spark for measurements of the fuel-to-air ratio of a combustible mixture, Fuel, 81: 1761-1765 (2002).

[21] A.E. Majd, A.S. Arabanian, R. Massudi, M. Nazeri, Spatially Resolved Laser-Induced Breakdown Spectroscopy in Methane-Air Diffusion Flames, Appl. Spectr., 65(1): 36-42 (2011).

[22] M.S. Bak, S. Im, M.G. Mungal, M.A. Cappelli, Studies on the stability limit extension of premixed and jet diffusion flames of methane, ethane, and propane using nanosecond repetitive pulsed discharge plasmas, Combust. Flame 160: 2396-2403 (2013).

[23] F. Cignoli, S. De Iuliis, V. Manta, and G. Zizak, Two-dimensional two-wavelength emission technique for soot diagnostics, Appl. Optics 40.30 (2001): 5370-5378.

[24] S. De Iuliis, F. Cignoli, and G. Zizak, (2006). Two-color laser-induced incandescence (2C-LII) technique for absolute soot volume fraction measurements in flames: erratum. Appl. Optics, *45*(16), 3805-3805.

[25] S. De Iuliis, F. Migliorini, F. Cignoli, and G. Zizak, (2007). 2D soot volume fraction imaging in an ethylene diffusion flame by two-color laser-induced incandescence (2C-LII) technique and comparison with results from other optical diagnostics. Proc. Combust. Inst., 31(1), 869-876.

[26] S. De Iuliis, F. Migliorini, F. Cignoli, and G. Zizak, (2006). Peak soot temperature in laser-induced incandescence measurements. Appl. Phys. B, 83(3), 397-402.

[27] G. De Falco, M. Commodo, A. D'Anna, and P. Minutolo, (2016). The evolution of soot particles in premixed and diffusion flames by thermophoretic particle densitometry. *Proceedings of the Combustion Institute in press* http://dx.doi.org/10.1016/j.proci.2016.07.108.

[28] D. Bradley, K.J. Matthews, J. Mech. Eng. Sci. 10: 299-304 (1968).

[29] G.P. Smith, D.M. Golden, M. Frenklach, N.W Moriarty, B. Eiteneer, M. Goldenberg, C.Th. Bowman, R.K. Hanson, S. Song, W.C. Gardiner Jr., V.V. Lissianski, and Z. Qin, http://www.me.berkeley.edu/gri_mech/index.html

[30] J.A. Miller, and C.F. Melius, Kinetic and thermodynamic issues in the formation of aromatic compounds in flames of aliphatic fuels. Combust. Flame 1992, 91(1), 21-39.

[31] N.M. Marinov, W.J. Pitz, C.K. Westbrook, M.J. Castaldi, and S.M. Senkan, Modeling of Aromatic and Polycyclic Aromatic Hydrocarbon Formation in Premixed Methane and Ethane Flames. Combust. Sci. Technol. 1996, 116-117(1-6), 211-287.

[32] H. Böhm, M. Braun-Unkhoff, and P. Frank, Investigations on initial soot formation at high pressures. Progr. Comp. Fluid Dynam. 2003, 3, 145-150.

[33] A. D'Anna, and A. Violi, A kinetic model for the formation of aromatic hydrocarbons in premixed laminar flames. Symposium (International) on Combustion 1998, 27(1), 425-433.

[34] M. Sirignano, J. Kent, A. D'Anna, Detailed modeling of size distribution functions and hydrogen content in combustion-formed particles. Combust. Flame 157 (6) (2010) 1211-1219.

[35] A. D'Anna, M. Sirignano, J. Kent, A model of particle nucleation in premixed ethylene flames, Combust. Flame 157 (11) (2010) 2106-2115.

[36] M. Sirignano, J. Kent, A. D'Anna, Modeling formation and oxidation of soot in nonpremixed flames, Energ. Fuel 27 (4) (2013) 2303–2315.

[37] M. Sirignano, and A. D'Anna, Further experimental and modelling evidences of soot fragmentation in flames, Proceedings of the Combustion Institute, (2015) 35: 1779-1786.

[38] R.J. Kee, F.M. Rupley, J.A. Miller, M.E. Coltrin, Grcar, et al., CHEMKIN Collection, Release 3.5, Reaction Design, Inc., San Diego, CA (1999).

[39] K. C. Smyth, J. H. Miller, R.C. Dorfman, W.G. Mallard, and R.J. Santoro, (1985). Soot inception in a methane/air diffusion flame as characterized by detailed species profiles. *Combustion and flame*, *62*(2), 157-181.

[40] C.J. Dasch, One-dimensional tomography: a comparison of Abel, onion peeling, and filtered backprojection methods, Appl. Opt. 31: 1146-152 (1992).

[41] L. Merotto, S. Dondè, and S. De Iuliis, LIBS and Chemiluminescence Measurements for Fuel/Oxidizer Mixing Monitoring, XXVIII Meeting of the Italian Section of the Combustion Institute, Lecce, Italy, September 20-23 2015. ISBN: 978-88-88104-25-6.